Review of International Geographical Education | RIGEO | 2020

RIGE

ISSN: 2146 - 0353

Review of International
GEOGRAPHICAL EDUCATION

www.rigeo.org

Thermal-Affected Zone Behavior in 13Cr-4Ni Martensitic Stainless Steel: A Simulation Study

PADMA RAO[1], NIHAL AHMED[2], Dr. SYED MUJAHED HUSSAINI[3]
Department of Mech
Nawab Shah Alam Khan College of Engineering and Technology (NSAKCET)

Abstract
There are a lot of things that happen when welding. Residual tensions cause the materials to undergo deformation. The process's significant temperature gradients are to blame for this propensity. Many experts in the field find these distortions very challenging. The purpose of establishing the behavior rules that will be used to analyze residual stresses and strains is to forecast these fluctuations. Welding processes in 13Cr-4Ni martensitic stainless steel are the subject of this investigation into the Thermal Affected Zone (TAZ). There is no change in the TAZ's knowledge of solid/liquid states. The only information it offers is about the austenite/martensite phase shift in metallurgy. This investigation makes use of three distinct categories of behavior laws: mechanical, thermal, and metallurgical. In order to assess the heat field that causes mechanical stresses, the thermal behavior law is used. The mechanical behavior law is used to assess the residual stress, which is composed of spherical stress (pressure) and deviatoric stress. Taking the whole strain into account is also useful. In order to assess the metallurgical phase proportions, the metallurgical behavior law is used. By running the simulations and comparing the outcomes with the analytical and experimental data, the models established in this work may be considered validated.

Keywords; Behaviour Laws, Martensitic Stainless Steel, Residual Stresses, Strain, Numerical Simulation

Introduction

These days, the metalworking sector is booming. The steel components are fabricated across the community. In the process of making the automobiles, they facilitate transportation. In addition to their wide range of uses, they are also present in several other systems. In the midst of all these uses, hydroelectric turbines are made. The Republic of the Congo is one of several nations that relies on energy to power its economy. Parameters such as water flow and turbine characteristics or quality determine the amount of energy produced at the hydroelectric power plant.
The 13Cr-4Ni martensitic stainless steel is used for the construction of hydroelectric turbines due to its exceptional corrosion resistance [1]. There is a second one that has to do with welding. Welding causes structural deformation of steel due to the significant temperature gradients that are present [2]. Fatigue performance, rigidity, and compressive stability are just a few of the mechanical qualities that are impacted by residual stresses and deformations during welding. Furthermore, fabrication accuracy and dimensional stability of welded structures are negatively impacted by welding deformation [3]. Predicting the strains caused by residual stresses is essential for ensuring a high-quality end result since these strains are permanent. Therefore, it is essential to have high-quality software to assist the industrialists with their tasks. In order to develop this software, it is necessary to model the equations that explain the welding-related behavior of the 13Cr-4Ni stainless steel. The article's main argument is this modeling.

To get the temperature field acting on the steel, one must first determine the thermal behavior law in the modeling part. The second step is to apply the mechanical behavior law to the temperature field in order to determine the strains and residual stresses. The third step in determining the metallurgical phase proportions is to propose the law of metallurgical behavior. The mechanical behavior of the welded components is affected by the metallurgical phases, which are austenite and martensite. Simulated findings will be compared to analytical and experimental data in order to resolve all of these

equations. Ansys will conduct all of the simulations. software version 18.1. The subjects of the research are limited to the TAZ, or Thermal Affected Zones. This means that the Fusion Zones (FZ) will not take into account the change of state (solid/liquid).

Properties of the 13Cr-4Ni Stainless Steel

Physical Properties

The 13Cr-4Ni is a martensitic stainless steel. This steel is very used for the man- ufacture of the hydroelectric turbines. The physical properties of 13Cr-4Ni are in Modelling of the Behaviour Laws

Thermal Behaviour Law

During the welding process, the welded pieces are under the effect of the high gradients of temperature. This phenomenon is not stationary in time. To deter- mine the value of the temperature T at any point of the material, the heat unsteady Equation (1) is applied.

$$\rho c \frac{dT}{dt} = -div(q) + W^{\square} \quad (1)$$

with:

ρc : heat capacity;

$\frac{dT}{dt}$: temporal derivative of T;

q: heat flux;

$W^{\square}$: coupling term, internal heat source.

One also considers that the material obeys the isotropic conduction law. So, the heat flux is defined by the Fourier Law (2).

$$q = -kgrad(T) \quad (2)$$

with:

k: conductivity of the material.

To solve this equation, the conditions on the boundary $\partial\Omega = \partial\Omega_1 + \partial\Omega_2 + \partial\Omega_3$ are specified. Three (3) types of boundary conditions are distinguished (**Figure 1**):

Convective and radiative condition on $\partial\Omega_1$. To write mathematically this condition, the two types of heat transfer modes are united by (3).

$$\begin{cases} h = h_{cv} + h_r \\ \text{with :} \\ h = \varepsilon \sigma (T + T_{ext})(T^2 + T_{ext}^2) \end{cases} \quad (3)$$

$$-kgrad(T)_s \cdot n_{ext} = h(T_s - T_{ext})$$

T_{ext}, T_s : exterior temperature, temperature at the surface;

n_{ext} : exterior normal to the surface;

ε_r : emissivity;

σ_r : Stefan constant = 5.66961×10^{-8} kg·s^{-3}·K^{-4};

h, h_{cv}, h_r : global transfer coefficients, convection coefficient, radiation coeffi- cient.

Dirichlet type condition with a set temperature $T = T_{imp}$ on $\partial\Omega_2$.

Or a Neumann type condition with a set flux such as

$-kgrad(T) \cdot n_{ext} = \varphi_{imp}$ on $\partial\Omega_3$.

Mechanical Behaviour Law

The mechanical modelling consists of establishing a behaviour law on which the values of the strains and residual stresses can be calculated. The mechanical be- haviour law must efficiently give in the TAZ the results near to the real solutions. It must be applied in a large range of temperatures. To evaluate the total strain ε, its decomposition to the diverse natures of strain is made. The separation is done on the basis of physical phenomena which operate during the welding process. So, there are the: elastic strain ε^{el}, viscop-

lastic strain ε^{vp} and thermal strain ε^{th}.

In the literature like [6], for the study of the steels welding behaviour, they add

ence of the formed metallurgical phases) and the transformation plasticity strain (due to the plasticity caused by the formed metallurgical phases). In this article, these two last types of strain are not considered because their influences are weak. So, one can write the mechanical behaviour law such as (4):

So, the different strains are:

Elastic Strain

The elastic strain is calculated by the Hooke Law:

ε^{el}

(5)

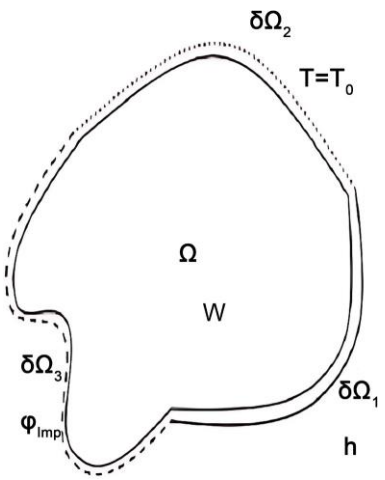

Figure 1. Boundary conditions of the thermal problem.

So, the equation of the elastic strain ε^{el} is such as:

$$\varepsilon^{el} = \frac{1+\nu}{E}\sigma - \frac{\nu}{E}tr(\sigma)\mathbf{I} + T\frac{\partial}{\partial T}\left(\frac{1+\nu}{E}\right)\sigma - T\frac{\partial}{\partial T}\left(\frac{\nu}{E}\right)tr(\sigma)\mathbf{I} \quad (6)$$

with:
ν : Poisson's ratio;
E: Young's modulus;
σ : stress.
By dividing the stress $\sigma = s - p\mathbf{I}$ to a deviatoric part s and a spherical one p (pressure), the following equations are obtained:

$$e^{el} = \frac{s}{2\mu} - T\frac{1}{2\mu^2}\frac{\partial \mu}{\partial T}s \quad (7)$$

$$tr\left(\varepsilon^{el}\right) = -\frac{p}{\chi} + T\frac{1}{\chi^2}\frac{\partial \chi}{\partial T} \quad (8)$$

e^{el} : deviatoric part of ε^{el};
μ : Lamé coefficient;
χ : hydrostatic compression modulus.
The Lamé coefficient μ and the hydrostatic compression modulus χ are given by:

$\mu = \frac{E}{2(1+\nu)}$,

$\chi = \frac{E}{3(1-2\nu)}$.

Thermal Strain

To establish the thermal strain, the mass conservation Equation (9) is used.

$$tr\left(\dot{\varepsilon}^{th}\right) = tr\left(\dot{\varepsilon}^{th}\right) = \nabla \cdot v = -\frac{1}{\rho}\frac{d\rho}{dt} \quad (9)$$

And the thermal tensor ε^{th} is considered as spherical such as (10):

$$\dot{\varepsilon}^{th} = -\frac{1}{3}\frac{d\rho}{d\rho}\mathbf{I} \quad (10)$$

The thermal strain rate is linked to the dilation coefficient α and the cool- ing speed $\dot{T}$ such as:

$$tr\left(\dot{\varepsilon}^{th}\right) = 3\alpha\dot{T} .$$

This leads to:

$$\dot{\varepsilon}^{th} = \alpha\dot{T}\,\mathbf{I} \quad (11)$$

Viscoplastic Strain

Perzyna [7] has defined a relation between the viscoplastic strain rate and the deviatoric stress s such as:

$$\dot{\varepsilon}^{vp} = \frac{3}{2\sigma}\left\langle \frac{\sqrt{-}}{-}\left\langle \frac{-}{\sqrt{3}} \right\rangle^{/} \right\rangle \quad (12)$$

$x = x$ si $\langle x \rangle$ $x \geq 0$,
$x = 0$ si $\langle x \rangle$ $x \leq 0$.

K: material consistency;
m: sensibility of the thermal stress.

There is a viscoplastic flow when the Von Mises stress is higher than the flow threshold σ_s. The equivalent stress σ acts like a tensile stress. In the results section, Equation (13) is used to compare this stress with the tensile stress de- veloped by the tensile test of a steel bar.

$$\sigma = \sigma + K\dot{\varepsilon}^{m(T)}\varepsilon^{n(T)} - \quad (13)$$

s

Metallurgical Behaviour Law

In the TAZ of the martensitic stainless steel 13Cr-4Ni, there are two phases: auste- nite during the heating and martensite during the cooling.

Austenitic Phase Proportion

To evaluate the austenitic phase proportion g_γ, W. Zhang [8] proposes the modified Avrami Equation (14).

γ 0

with:

$i=1$ $\left(\quad _i \right)$

E_a : transformation apparent activation energy;

k_0, n : parameters;

R: ideal gas constant;

T_i : temperature at initial instant t_i ;

m_i : number of increments.

In this study, the values of these above cited parameters are given in **Table 3** like presenting by J.B. Levesque [5].

To validate the austenitic phase proportion g_γ , the results obtained will be compared with the experimental values found by J.B. Levesque [5].

Martensitic Phase Proportion

Van Bohemen *et al.* [9] have studied the influence of chemical composition on the martensitic phase proportion. They have proposed the Equation (15) to eva- luate the martensitic phase proportion by using the chemical composition and the temperature.

$$g_{\alpha'} = 1 - \exp\left(-a_m \left(T_{KM} - T\right)\right) \qquad (15)$$

with:

T_{KM} : temperature at the beginning of martensitic transformation;

a_m : parameter of transformation rate;

T: temperature of the material.

The authors have defined T_{KM} and a_m as follow:

$$T_{KM} = 462 - 273x_C - 26x_{Mn} - 16x_{Ni} - 13x_{Cr} - 30x_{Mo} \qquad (16)$$

$$a_m = 0.0224 - 0.0107x_C - 0.0007x_{Mn} - 0.00005x_{Ni} - 0.00012x_{Cr} - 0.0001x_{Mo} \qquad (17)$$

The chemical atom proportion x of the 13Cr-4Ni stainless steel, S41500, is given in **Table 2**. The values found by J.B. Levesque are used to make the comparison with the results of this study.

Results and Discussion

All the equations of the modelling section are implemented in ANSYS 18.1 soft- ware to get the results presented in this section.

Validation of the Mechanical Behaviour Law

Elasto-Viscoplastic Strain: Tensile Test

To validate or verify the correctness of the elasto-viscoplastic strain term in the mechanical behaviour law, the tensile test is made. As specified in Section 3.2.3, viscoplastic stress acts like tensile stress. So, the Von Mises equivalent stress (ten- sile stress) is given by (18).

$$\sigma = \sigma - \sigma = K\varepsilon^{m(T)}\dot{\varepsilon}^{n(T)} \qquad (18)$$

By Equation (18), the analytical values are compared with the numerical ones found by the tensile test with ANSYS 18.1. The physical parameters for the analytical calculus are given in **Table 1**.

Table 1. Parameters of the simulation.

E_a	k_0	n
509.9 KJ·mol^{-1}	4.04 × 10^{24}	0.66

Table 2. Mechanical parameters of 13Cr-4Ni steel [4].

K (MPa·s^{-1})	m	n	σ_s (MPa)	ν	E (GPa)
252	0,3	0.35	20	0.288	206

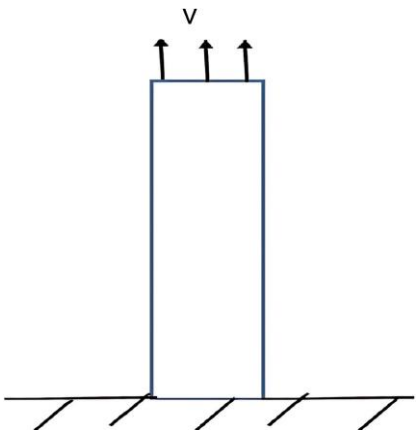

Figure 2. Geometry of the cylindrical bar in the tensile test.

The analytical and the numerical values of the experiment are presented in **Fig- ure 3**.
By **Figure 1**, the numerical values are near to the analytical ones. So, the mod- elling conceived is correct.

Thermal Strain

To validate the expression of the thermal strain in the mechanical behaviour law, the thermal loading on ANSYS 18.1 is made. So, a cylindrical bar of length 0.1 m

and 0.1 m of radius is used. A progressive heat source of temperature $T(t)$ variable in the time is applied. The Temperature increases by 5°C·s^{-1}. The cylindrical bar is fixed between two trays. The experiment is done during $t = 20\,\text{s}$.
The time step is $\Delta t = 0.1\,\text{s}$.
The analytical expression of thermal strain is given by (19).

$$\sigma^{th} = E\varepsilon^{th} = \alpha ET\square t \quad (19)$$

Figure 2 shows the comparison between the analytical (gray) and the numer- ical values (orange) obtained. The results found are near. The coherence of re- sults is found.

Validation of the Thermal Behaviour Law

Kondrashov [10] proposes an analytic solution of the heat equation for the non-isothermal transformations with a Neumann type condition. This solution

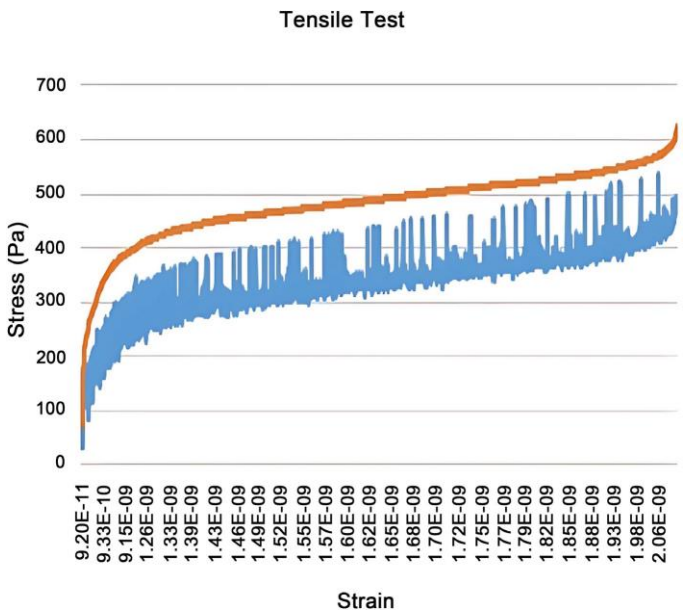

Figure 3. Tensile test, analytical results (orange), numerical results (blue).

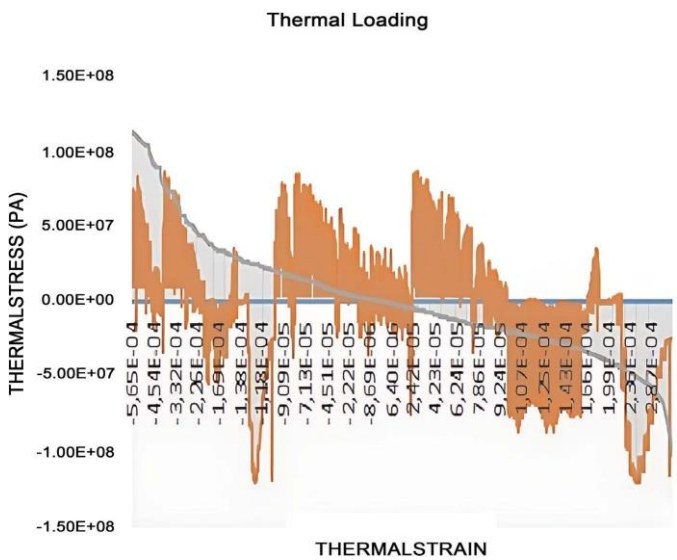

Figure 4. Thermal stress.

is used for comparing the numerical solution, implemented by ANSYS 18.1, with this analytic one. The analytic solution of the heat equation is given by (20).

$$T(x,t) = T_0 + (T_s - T_0)\,\mathrm{erf}\left(\frac{x}{2\sqrt{\alpha_s t}}\right) + (T_s - T_0)\,\frac{\sqrt{\alpha_s t}}{k}\,\mathrm{erf}\left(\frac{x}{2\sqrt{\alpha_s}}\right) \quad (20)$$

$$T(t=0)=T_i\ T(x=0)=T_0\ T(x=\infty)=T_i$$

$$T_s=T\left(x=x_s=k_s\sqrt{t}\right).$$

α_s : thermal diffusivity;
k_s : thermal conductivity;
x_s : solidus position or limit of the TAZ;
T_s : solidus.

$erf(X)$ is the Gauss error function. It is defined as follows:

$$erf(X)=\frac{2}{\sqrt{\pi}}\int_0^X \exp\left(-u^2\right)du \quad (21)$$

So:

$$erf\left(\frac{x}{2\sqrt{\alpha_s t}}\right)=\frac{2}{\sqrt{\pi}}\left(-\frac{x^2}{4\alpha_s t}\right)\left(-\frac{x}{2\sqrt{\alpha_s t}}\right)+\frac{4}{\sqrt{\pi}}\exp\left(-\frac{x^2}{4\alpha_s t}\right)+\frac{(22)}{\sqrt{\pi}}$$

$$erf\left(\frac{k_s}{2\sqrt{t}}\right)=\frac{2}{\sqrt{\pi}}\left(-\frac{k_s}{2\alpha_s}+\frac{k_s}{2\sqrt{\alpha_s}}-2\right)\exp\left(-\frac{k_s}{4\alpha_s}\right)+\frac{4}{\sqrt{\pi}}+\frac{(23)}{\sqrt{\pi}}$$

To solve numerically the heat Equation (1), a 2D bar 1 × 50 mm² is considered.
The initial temperature of the material is $T_i=1650$ °C. The temperature at the left limit is suddenly reduced to 800°C. The time step is $dt=0.1\,\text{s}$ and the space step is $dx=dy=0.5\,\text{mm}$. The simulation is made during $t=20\,\text{s}$. **Figure 5** shows the profile of temperature in the bar during the simulation.
The analytic (black color) and numerical (blue color) results obtained are pre- sented in **Figure 6**. The two results are numerically near. So, the correctness of the results is found.

Validation of the Metallurgical Behaviour Law

Martensitic Phase Simulation

On the basis of the metallurgical phase proportion modelling, the martensitic phase proportion is obtained. The curve presenting this evolution is given in **Figure 7**.
The numerical solution is compared with the experimental data found by J.B. Levesque [5]. The evolution of the experimental curve is given in **Figure 8**.

Austenitic Phase Simulation

The numerical austenitic phase proportion, found on the basis of the modelling developed in Section 3.3, is given in **Figure 9**.
The values found by the simulation are compared with the experimental data [5] (**Figure 10**). So, the correctness of the results is found.

Conclusion

In this article, the thermal, mechanical and metallurgical behaviour laws in the

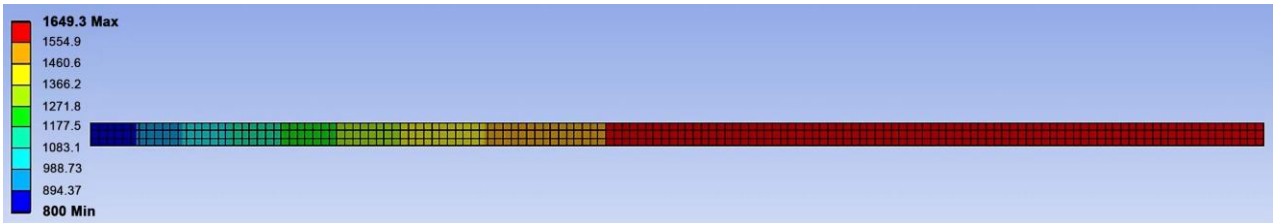

Figure 5. Temperature profile in the bar.

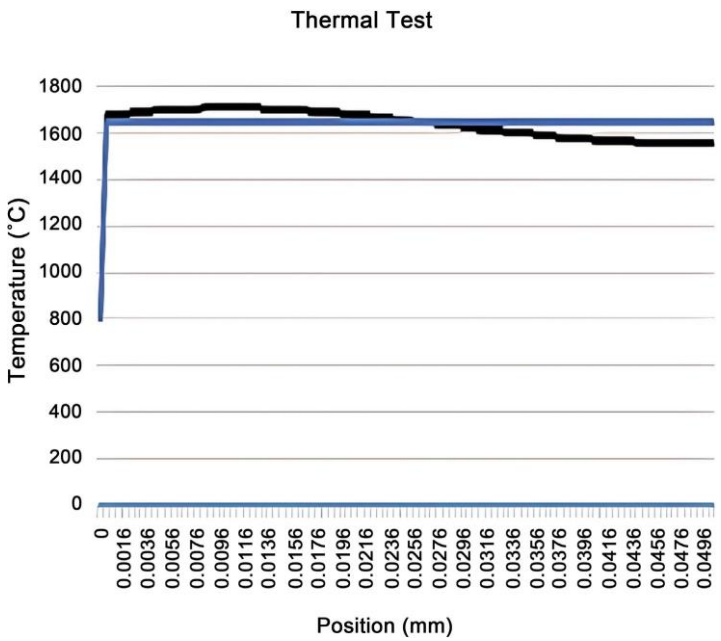

Figure 6. Analytical (black) and numerical (blue) results.

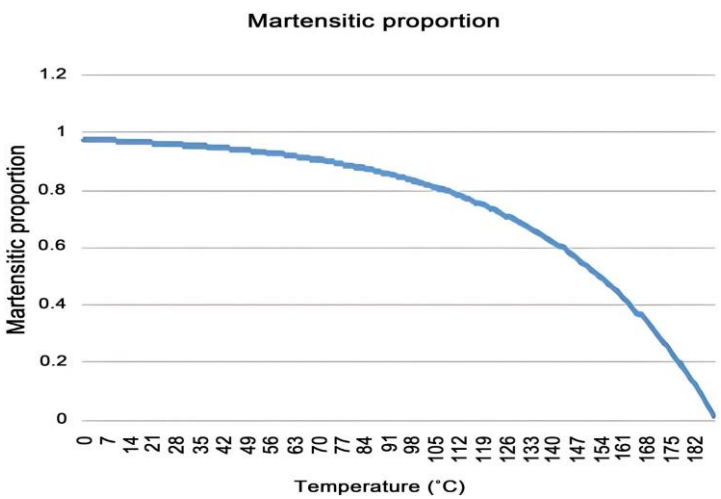

Figure 7. Martensitic phase proportion by numerical simulation.

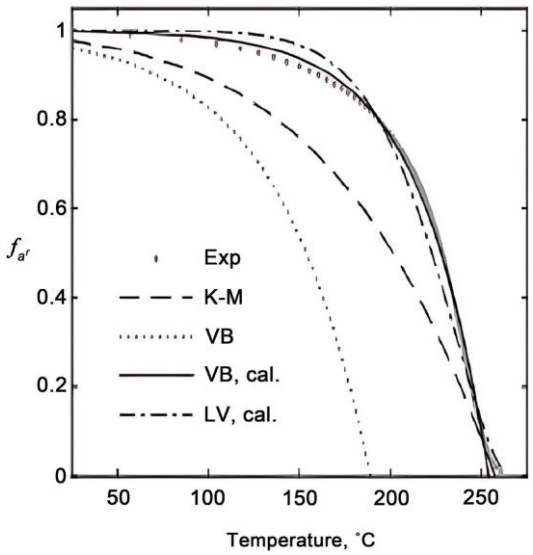

Figure 8. Martensitic phase proportion by experi- mental data extracted from [5].

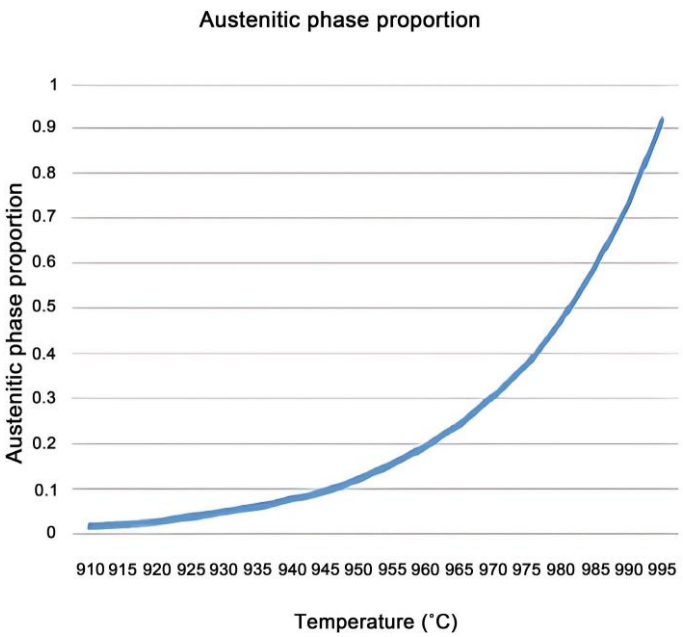

Figure 9. Austenitic phase proportion by numerical simulation.

TAZ of the 13Cr-4Ni stainless steel are presented. The mechanical behaviour law serves to evaluate the strains and residual stresses. So, to evaluate the stresses and the strains during the welding, some equations are developed. To validate these equations, one has confronted their numerical results with the analytic or experimental data. One has made the same for the thermal and metallurgical behaviour laws. The thermal modelling is based on the heat equation. The me- tallurgical behaviour law focuses on the solid-state phase proportions (marten- site and austenite). The results obtained show the correctness of the modelling. The future research directions on the simulation of the welding must take into

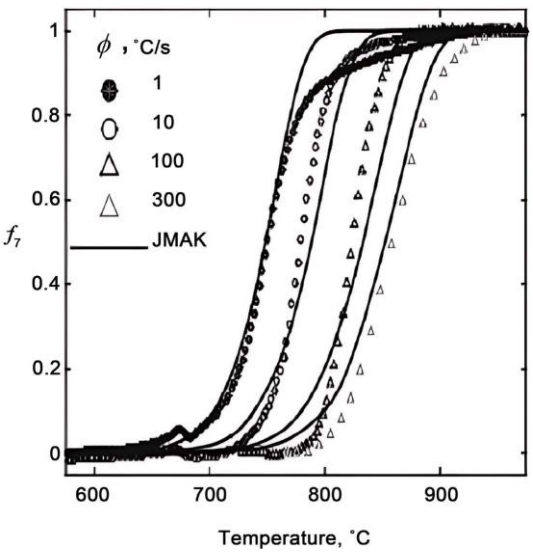

Figure 10. Austenitic phase proportion by experi- mental data extracted from [5].

account the prediction of the fissure formation. The fissuring is a real problem during the welding which influences the material stability.

Conflicts of Interest

The authors declare no conflicts of interest regarding the publication of this pa- per.

References

First cited in McGuire, M. (2008), Stainless Steels for Environmental Engineers. In the United States of America, at ASM International's Materials Park. The World Health Organization website

[2] Research on the Effect of Heat Treatment on the Hardness of 13Cr-4Ni-(Mo) (F6NM) Steel Grade for Use in Industrial Heats by De Sanctis, Buccioni, Donato, Richetta, and Varone (2017). Article 351 of Metals, Volume 7, Section 7. This article is cited as https://doi.org/10.3390/met7090351.

According to Sonsimo (2008), fatigue behavior of welded joints is affected by residual stresses, which vary with loading conditions and weld geometry. Journal of Fatigue Research, 31, 88-101. Here is the link to the article: https://doi.org/10.1016/j.ijfatigue.2008.02.015. A

[4] Low Alloy Steel Materials Overview (Matweb, 2023). Here is the link to the datasheet: https://www.matweb.com/search/1

Metallurgical and Materials Transactions A, 51, 1208-1220, Levesque, J.B., Lanteigne, J., Champliaud, H., and Paquet, D. (2020) Modeling Sol-id-State Phase Transformations of 13Cr-4Ni Steels in the Welding Heat-Affected Zone. URL: https://doi.org/10.1007/s11661-019-05587-1

Interactions between stresses and diffusive phase transformations with plasticity were discussed by Gautier (1997) in reference 6. Mechanics of Solids with Phase Changes, edited by Berveiller and Fischer, F.D. Publishing House: Springer, Vienna, International Centre for Mechanical Sciences, 105–120. You can access the article at this link: https://doi.org/10.1007/978-3-7091-2660-8_4.

[7] In a 2002 study, Helferes, O.M., Suiker, A.S.J., and de Borst, R. A Study Contrasting the Per-zyna and Consistency Viscoplastic Models. The European Journal of Published in Mechanics, volume 21, pages 1-12, with the DOI 10.1016/S0997-7538(01)01188-3.

In their 2002 paper, Zhang, Elmer, and Debroy modeled and mapped the phases of GTA welding of 1005 steel in real time. Article 333, pages 320-335 in Materials Science and Engineering. This resource can be found at this URL: https://doi.org/10.1016/S0921-5093(01)01857-3.

According to a study by Van Bohemen and Sietsma (2009), the kinetics of athermal martensite formation in plain carbon steels are affected by composition. Volume 25, Issue 10, Pages 1009–1012, Society for Materials Science and Technology. In order to access the article, go to https://doi.org/10.1179/174328408X365838.

In the International Journal of Heat and Mass Transfer, Kondrashov (2009) presented an analytical solution to the one alloy solidification problem. The paper may be found in volume 52, pages 67–69. The link to the article is https://doi.org/10.1016/j.ijheatmasstransfer.2008.05.027-.